

A Scalar-on-Quantile-Function Approach for Estimating Short-term Health Effects of Environmental Exposures

Yuzi Zhang * ¹, Howard H. Chang¹, Joshua L. Warren², and Stefanie T. Ebelt³

¹Department of Biostatistics and Bioinformatics, Emory University, Atlanta, GA, USA

²Department of Biostatistics, Yale University, New Haven, CT, USA

³Department of Environmental Health, Emory University, Atlanta, GA, USA

Abstract

Environmental epidemiologic studies routinely utilize aggregate health outcomes to estimate effects of short-term (e.g., daily) exposures that are available at increasingly fine spatial resolutions. However, areal averages are typically used to derive population-level exposure, which cannot capture the spatial variation and individual heterogeneity in exposures that may occur within the spatial and temporal unit of interest (e.g., within day or ZIP code). We propose a general modeling approach to incorporate within-unit exposure heterogeneity in health analyses via exposure quantile functions. Furthermore, by viewing the exposure quantile function as a functional covariate, our approach provides additional flexibility in characterizing associations at different quantile levels. We apply the proposed approach to an analysis of air pollution and emergency department (ED) visits in Atlanta over four years. The analysis utilizes daily ZIP code-level distributions of personal exposures to four traffic-related ambient air pollutants simulated from the Stochastic Human Exposure and Dose Simulator. Our analyses find that effects of carbon monoxide on respiratory and cardiovascular disease ED visits are more pronounced with changes in lower quantiles of the population's exposure. Software for implement is provided in the R package nbRegQF.

Keywords: Air pollution, Bayesian hierarchical modeling, Functional data analysis, Quantile process

*yuzi.zhang@emory.edu

1 Introduction

Environmental epidemiological studies routinely utilize aggregate health data to assess short-term health effects of environmental exposures. For example, city-wide daily counts of deaths, emergency department (ED) visits, and preterm births have been linked to short-term exposure to air pollution and extreme temperature (Alhanti et al., 2016; Guo et al., 2017; Bekkar et al., 2020; Yoo et al., 2021). The use of aggregate health data represents an ecological design, where the true exposure corresponds to the distribution of individual-level exposure across the at-risk population (Richardson and Best, 2003; Sheppard, 2003). However, individual environmental exposures cannot be practically measured in large population-based studies. Instead, exposure surrogates that reflect summaries of individual-level exposure (e.g., the mean) are used. This can result in exposure misclassification that leads to biases and incorrect characterization of uncertainties associated with the health effect estimates (Dominici et al., 2000; Richmond-Bryant and Long, 2020).

In the context of air pollution, ambient pollutant levels are frequently the exposure of interest so that regulatory policies may be developed. Within short-term time-scales of interest, there can be considerable exposure heterogeneity within the population since (1) air pollutants can exhibit spatial variation within the study region, and (2) individuals spend most of their time in different indoor environments, each with unique outdoor to indoor pollution infiltration characteristics. To address the first challenge, spatial-temporal models have been developed to estimate pollutant concentrations at fine spatial resolutions that can provide complete spatial-temporal coverage (Jerrett et al., 2001, 2005). Population-weighting is then used to construct short-term exposure values to link with aggregated health outcome data, over spatial units of interest (e.g., ZIP code). Accounting for spatial exposure variability within temporal studies has been shown to result in larger health effect

estimates compared to the use of exposure metrics measured by sparse, stationary monitors, especially for pollutants with high degrees of spatial variability (e.g., traffic-related pollutants) (Goldman et al., 2010; Sarnat et al., 2013).

In contrast, less work has been done to address exposure heterogeneity due to individual time spent in different microenvironments. With the development of wearable devices, personal exposure to environmental contaminants can be more easily measured (Steinle et al., 2013, 2015; Sugg et al., 2018). While the cost is prohibitive for population-based epidemiological studies, findings from small exposure assessment studies have been used to develop probabilistic models to simulate population-level distributions of personal exposures, incorporating time-activity-location patterns and parameters describing the relationships between ambient and indoor environments. When spatially-refined ambient exposure is used as an input, the resulting simulated personal exposure distributions reflect both spatial heterogeneity in ambient concentrations and population heterogeneity in time-activity-location patterns. Examples of probabilistic models include pCNEM and the Stochastic Human Exposure and Dose Simulation (SHEDS) (Burke et al., 2001; Zidek et al., 2005, 2007), as well as a statistical emulator to reduce the computational burden for large-scale epidemiological studies (Chang et al., 2012).

With simulated personal exposures from such probabilistic models, previous studies of aggregate health outcomes have used exposure distribution summary statistics (e.g., daily mean or median) as the covariate in the health model (Calder et al., 2008; Chang et al., 2012; Sarnat et al., 2013). However, ecological bias is still present because the daily mean of personal exposures does not fully capture heterogeneity of exposures experienced by the population (Sheppard, 2003). For example, in the special case where personal exposures are normally distributed, inclusion of exposure variance in the health model can result in

unbiased estimates (Sheppard, 2003; Reich et al., 2009). However, the population distribution of environmental exposure is often skewed and poorly approximated by a normal distribution (Leiva et al., 2008; Huang et al., 2018). Furthermore, all previous methods using population summary statistics implicitly assume that the health effect of air pollution can be entirely characterized by the summary statistic selected. In other words, health risks only depend on changes in that selected summary statistic. However, health risks may also depend on changes in the exposure distribution that cannot be reflected by changes in the selected summary statistic. For example, consider a scenario where a short-term increase in air pollution may be more detrimental to individuals who are typically exposed to lower pollution levels. For such scenario, an increase in the lower tail of population-level exposure results in larger increases in the risk of adverse health events, while solely including the population-level mean exposure is insufficient to fully characterize the exposure-response relationship.

In this work, we propose a general modeling framework to incorporate within-unit population-level exposure heterogeneity via exposure quantile functions. Instead of only using unit-level population-average or variance, exposure quantile functions comprehensively summarize the entire within-unit exposure distribution throughout the study. In our framework, the exposure quantile function is viewed as a functional covariate with respect to quantile levels. Therefore, we further allow effects of exposure at different quantile levels to vary. Estimation and inference are carried out under a Bayesian hierarchical modeling framework that also propagates uncertainties associated with the estimation of exposure quantile functions into the health effect estimate.

2 Motivating Data and Application

Ambient air pollution exposure has been identified as a risk factor of various diseases (Lan-drigan, 2017; Manisalidis et al., 2020), contributing significantly to global disease burden (Boogaard et al., 2019). Here we studied short-term associations between daily ED visits and ambient air pollution exposures in a time-series design (Bhaskaran et al., 2013). We obtained daily counts of ED records during the period January 1st, 1999 - December 31st, 2002 in Atlanta. Counts were also stratified by one on the 40 ZIP code tabulation areas (ZCTAs). We analyzed three causes for ED visits identified using International Classification of Diseases 9th Revision (ICD-9) diagnosis code: (1) respiratory disease (ICD-9 codes: 460-465, 466.0, 477, 466.1, 466.11, 466.19, 480-486, 491-493, 496, 786.07), (2) a subset of respiratory diseases which only includes asthma or wheeze (ICD-9 codes: 493, 786.07), and (3) cardiovascular disease (ICD-9 codes: 410-414, 427-428, 433-437, 440, 443-445, 451-453).

We examined four traffic-related air pollutants: particulate matter with aerodynamic diameter < 2.5 microns ($PM_{2.5}$), carbon monoxide (CO), nitrogen oxides (NO_x), and elemental carbon (EC), a constituent of $PM_{2.5}$. Separately for each pollutant, population-level distributions of personal exposure were obtained from SHEDS model (Burke et al., 2001). This model is a stochastic simulator producing daily personal exposure at the census tract level (Özkaynak et al., 1996; Jenkins, 1996; Dionisio et al., 2013). To estimate the personal exposure distributions of ambient concentrations of an air pollutant, the SHEDS model first simulates exposures for multiple hypothetical individuals for each census tract that reflect the demographic characteristics (e.g., age, sex, work locations) of the at-risk population using Census data. The amount of time each hypothetical individual spends in various microenvironments is obtained by randomly assigning an activity diary from the US Environmental Protection Agency (EPA)’s Consolidated Human Activity Database based on

their demographics. Their daily personal exposure is then computed by summing time-weighted average exposure across all thirteen microenvironments that are categorized into four types (outdoors, vehicle, residential indoors, and non-residential indoors microenvironments). For this analysis, the personal exposure distribution at the census tract level were then aggregated to the ZCTA level.

For the health analysis, several meteorological variables were obtained from Daymet to account for potential confounding by meteorology (Thornton et al., 2016). These include daily minimum temperature, maximum temperature, and dew-point temperature.

3 Method

3.1 Model for count outcome and mean exposure

We first describe the conventional log-linear model for aggregate outcomes. Let y_i denote the number of events (e.g., ED visits, hospital admissions, deaths) observed for group $i = 1, \dots, n$, and let $\mathbf{x}_i = (x_{i1}, \dots, x_{im_i})^T$ denote a vector of exposures (e.g., personal exposures to air pollution) collected from m_i individuals for group i . A group can be formed by geographical areas or a time interval. In most applications, the mean of the group-specific exposures are used in an over-dispersed Poisson log-linear regression model such as:

$$Y_i | \lambda_i \sim \text{Poisson}(\lambda_i), \quad \lambda_i | \xi, \eta_i \sim \text{Gamma}(\xi, \exp(\eta_i)), \quad \text{and} \tag{1}$$

$$\eta_i = \alpha \mu_i + \boldsymbol{\gamma}^T \mathbf{Z}_i + \epsilon_i,$$

where μ_i denotes the true mean exposure of group i often estimated by the sample average $\sum_{j=1}^{m_i} x_{ij} / m_i$, parameter α represents the effect of the mean exposure, \mathbf{Z}_i is a vector of other covariates with regression coefficients $\boldsymbol{\gamma}$ (including an intercept), ξ controls the amount of

over-dispersion, and ϵ_i represents a mean-zero spatial/temporal residual process. Using this parametrization, the log of the expectation of Y_i equals to $\log(\xi) + \eta_i$. Model (1) only depicts the association between expected health outcome count and population-wide mean exposure which ignores exposure heterogeneity among individuals. Therefore, model (1) may be an insufficient framework to characterize effects of exposure on health. For example, model (1) fails to capture health effects associated with changes in exposure distributions having same population-wide means.

3.2 Model for count outcome and exposure distribution

To capture effects of the entire exposure distribution and to allow effects to vary by quantile levels, we propose a model treating exposure quantile functions as functional covariates. The proposed scalar-on-quantile-function over-dispersed Poisson log-linear regression model is given as:

$$Y_i | \lambda_i \sim \text{Poisson}(\lambda_i), \quad \lambda_i | \xi, \eta_i \sim \text{Gamma}(\xi, \exp(\eta_i)), \quad \text{and} \quad (2)$$

$$\eta_i = \int_0^1 \beta(\tau) Q_i(\tau) d\tau + \boldsymbol{\gamma}^T \mathbf{Z}_i + \epsilon_i,$$

where $Q_i(\cdot)$ denotes the exposure quantile function of a continuous exposure for group i . Note that $\beta(\tau)$ represents the effect of the exposure's τ -th percentile on the mean of the health outcome while other parameters were previously described in model (1).

To flexibly characterize the association between health outcome and the exposure, the coefficient $\beta(\tau)$ is assumed to be a smooth function of quantile levels and is modeled via a finite number of basis functions. Specifically, $\beta(\tau)$ is specified as:

$$\beta(\tau) = \sum_{j=0}^p K_{j,p}(\tau) \beta_j, \quad (3)$$

where $K_{j,p} = \left(\sqrt{2(p-j)+1}\right)(1-\tau)^{p-j} \sum_{k=1}^j (-1)^k \binom{2p+1-k}{j-k} \binom{j}{k} \tau^{j-k}$ denotes the orthonormal Bernstein polynomials of degree p defined over the interval $[0, 1]$ (Bellucci, 2014). With this basis expansion, the proposed model in Eqn. (2) can be written as:

$$\eta_i = \boldsymbol{\beta}^T \int_0^1 \mathbf{K}(\tau) Q_i(\tau) d\tau + \boldsymbol{\gamma}^T \mathbf{Z}_i + \epsilon_i, \quad (4)$$

where $\boldsymbol{\beta} = (\beta_0, \dots, \beta_p)^T$ is a vector of basis coefficients and $\mathbf{K}(\tau) = (K_{0,p}(\tau), \dots, K_{p,p}(\tau))^T$ is a vector of basis functions. We note that the domain of Bernstein polynomials coincides with the domain of exposure quantile functions, which could facilitate the estimation of $\boldsymbol{\beta}$, compared to B-splines or Gaussian kernels. The Bernstein polynomials are chosen also because they have been shown to accurately approximate various smooth function forms with a small number of basis functions (Bellucci, 2014). We note one special case where effects of exposure are the same at different quantile levels (i.e., $\beta(\tau)$ is a constant in τ). Then the proposed model (2) will reduce to model (1) because $\int_0^1 Q_i(\tau) d\tau = \mu_i$.

3.3 Estimation and inference

3.3.1 Quantile functions are known

With known quantile functions, Eqn. (4) can be reparametrized as a regular scalar-on-scalar model with a covariate vector $\mathbf{X}_i^* = \int_0^1 \mathbf{K}(\tau) Q_i(\tau) d\tau$. For example, in Reich et al. (2009), $Q_i(\tau)$ is assumed to be Normal quantile functions. An efficient fully Bayesian inference procedure is available for the over-dispersed Poisson regression by introducing latent Polya-Gamma random variables (Polson et al., 2013; Neelon, 2019). Using the Polya-Gamma method, coefficients $\boldsymbol{\beta}$ and $\boldsymbol{\gamma}$ can be estimated via Markov Chain Monte Carlo (MCMC) using Gibbs sampling. With independent normal priors introduced for coefficients $\boldsymbol{\beta}$ and

γ , the full conditional distribution for those regression coefficients is a multivariate normal distribution.

3.3.2 Quantile functions are unknown

For the more realistic case of unknown quantile functions, we propose a two-stage Bayesian estimation procedure. In the first stage, quantile function $Q_i(\tau)$ for each group i is again modeled using basis expansion and estimated from individual-level exposures (e.g., SHEDS simulations in our application). In the second stage, the health model (2) is fitted with estimated quantile functions while accounting for the statistical uncertainties associated with the first-stage estimation.

Following previous semiparametric Bayesian approaches for modeling quantile processes for continuous variables (Reich, 2012), the quantile function for exposures in group i is expanded as:

$$Q_i(\tau) = \theta_{0,i} + \sum_{l=1}^L B_l(\tau)\theta_{l,i}, \quad (5)$$

where $B_l(\tau)$ is the l -th basis function, and $\theta_{l,i}$ are basis coefficients. Choices of basis function $B_l(\tau)$ include piecewise Gaussian or piecewise Gamma functions, and their expressions are provided in supplementary materials. Both choices permit us to flexibly characterize the potentially skewed distribution of exposures. However, for exposures that are strictly positive (e.g., ambient air pollution concentration), piecewise Gamma functions are recommended. With the use of piecewise Gaussian or Gamma functions, $\theta_{0,i}$ represents the median of the i -th group exposure distribution and $\theta_{l,i}$ for $l = 1 \dots, L$ characterize the shape of the distribution. The quantile function uniquely defines the density. Let x_{ij} denote the exposure level measured for the j -th individual within the i -th group. When x_{ij} is assumed to follow a distribution corresponding to a quantile function $Q_i(\tau)$, the likelihood

for a set of individual-level exposures is given by

$$L(\boldsymbol{\theta}_{0,\cdot}, \{\boldsymbol{\theta}_{l,\cdot}\}_{l=1}^L; \{\mathbf{x}_i\}_{i=1}^n) = \prod_{i=1}^n \prod_{j=1}^{m_i} \left[\frac{dQ_i(\tau)}{d\tau} \right]^{-1} \Big|_{\tau^*: Q_i(\tau^*)=x_{ij}}, \quad (6)$$

where $\boldsymbol{\theta}_{0,\cdot} = (\theta_{0,1}, \dots, \theta_{0,n})^T$, $\boldsymbol{\theta}_{l,\cdot} = (\theta_{l,1}, \dots, \theta_{l,n})^T$, and $\mathbf{x}_i = (x_{i1}, \dots, x_{im_i})^T$ is a vector of personal exposures collected for group i of m_i individuals. It is important to note that quantile functions have to be non-decreasing. To ensure this property, $\theta_{l,i} > 0$ should hold for any i and l (Reich, 2012). In the first-stage estimation, this constraint is imposed by introducing an unconstrained latent variable $\theta_{l,i}^*$. Specifically, $\theta_{l,i} = \max\{\theta_{l,i}^*, \nu\}$, where ν is a small constant (e.g., 0.01). For spatial or time-series data, one can easily introduce spatial or temporal dependence for $\boldsymbol{\theta}_{0,\cdot}$ and $\boldsymbol{\theta}_{l,\cdot}^* = (\theta_{l,1}^*, \dots, \theta_{l,n}^*)^T$ in the Bayesian hierarchical modeling framework to allow quantile processes to vary by time or locations. Estimation of all model parameters is carried out via MCMC algorithms.

In the second-stage, the health model is fitted while accounting for the uncertainties associated with estimating exposure quantile functions. When the exposure quantile function is expanded using basis functions, the health model in Eqn. (4) becomes:

$$\eta_i = \boldsymbol{\beta}^T \left[\int_0^1 \mathbf{K}(\tau) \mathbf{B}(\tau)^T d\tau \right] \boldsymbol{\theta}_{\cdot,i} + \boldsymbol{\gamma}^T \mathbf{Z}_i + \epsilon_i, \quad (7)$$

where $\mathbf{B}(\tau) = (1, B_1(\tau), \dots, B_L(\tau))^T$ and $\boldsymbol{\theta}_{\cdot,i} = (\theta_{0,i}, \theta_{1,i}, \dots, \theta_{L,i})^T$. Since $\mathbf{B}(\tau)$ is pre-specified, uncertainties of estimated $\boldsymbol{\theta}_{\cdot,i}$, contribute to uncertainties of the estimation of quantile functions.

To appropriately propagate uncertainties resulting from the first-stage estimation, we consider an approach which is commonly used in environmental health studies for incorporating uncertainties in estimated exposures (Carroll et al., 2006; Lee et al., 2017). Specif-

ically, a multivariate normal (MVN) prior is assumed for $\boldsymbol{\theta}_{.,i}$ with mean and variance-covariance matrix computed from its posterior predictive distribution obtained from the first-stage estimation. Similarly to the case in which quantile functions are known, we view $\mathbf{X}_i^* = [\int_0^1 \mathbf{K}(\tau)\mathbf{B}(\tau)^T d\tau]\boldsymbol{\theta}_{.,i}$ as a random covariate vector. With MVN prior assumed for $\boldsymbol{\theta}_{.,i}$, the prior of \mathbf{X}_i^* is also MVN. It is worth noting that posterior distributions of $\boldsymbol{\theta}_{.,i}$ are correlated across groups when quantile processes are assumed to vary by groups. As the number of groups increases, this approach becomes computational expensive since the MCMC algorithm requires sampling from a high-dimensional MVN distribution. In the simulation study and real data analysis, we ignore the correlation between groups to facilitate the computation. We find that this does not meaningfully impact inference for the health effect association, as also recently demonstrated in Comess et al. (2022). As in the case of known quantile functions, the estimation of coefficients $\boldsymbol{\beta}$ and $\boldsymbol{\gamma}$ is carried out by Gibbs sampling with normal priors specified for those coefficients using the Polya-Gamma method. Details of MCMC algorithms for the estimation of quantile functions, and the estimation with known and unknown quantile functions can be found in the supplementary materials.

4 Simulation Studies

We conducted simulation studies to examine the impact of not accounting for exposure heterogeneity motivated by our application and evaluated the performance of the two-stage estimation procedure. A variety of associations between exposures and outcomes are considered by specifying different forms of coefficient regression function $\beta(\tau)$.

The simulation study assumes that health outcome is collected over $n = 1000$ time points and exposure quantile functions are temporally correlated. The temporal depen-

dence was introduced by defining a first-order Gaussian Markov random field process for the unconstrained latent basis coefficients. The true health model and exposure quantile function are:

$$Y_i | \lambda_i \sim \text{Poisson}(\lambda_i), \quad \lambda_i | \xi, \eta_i \sim \text{Gamma}(\xi, \exp(\eta_i)),$$

$$\eta_i = \beta_0 + \int_0^1 \beta(\tau) Q_i(\tau) d\tau, \quad i = 1, \dots, 1000,$$

$$Q_i(\tau) = \theta_{0,i} + \sum_{l=1}^4 B_l(\tau) \theta_{l,i},$$

$$(\theta_{0,1}, \dots, \theta_{0,1000})^T \sim \text{MVN}(\theta_0, \Sigma_0), \quad \Sigma_0 = \sigma_0^2 (D_w - \rho_0 W)^{-1},$$

$$(\theta_{l,1}^*, \dots, \theta_{l,1000}^*)^T \sim \text{MVN}(\theta_l, \Sigma_l), \quad \Sigma_l = \sigma_l^2 (D_w - \rho_l W)^{-1} \text{ for } l = 1, \dots, 4, \theta_{l,i} = \max\{\theta_{l,i}^*, \nu = 0.01\},$$

where $B_l(\tau)$ are piecewise Gamma functions with 4 basis functions; W is a symmetric matrix with the (i, i') entry equal to 1 if time point i and i' are adjacent, and 0 otherwise; and D_w is a diagonal matrix with the i -th diagonal element equal to the row sum of i -th row of W . For each time point i , individual exposure data with a sample size of 100 were generated using the quantile function $Q_i(\tau)$. To mimic the right-skewed distribution of $\text{PM}_{2.5}$ observed in the motivating data, we set $\theta_0 = 7.2$, $\theta_l = 0.9$ for $l = 1, \dots, 4$, and parameters controlling temporal correlations of quantile processes $(\sigma_0^2, \rho_0, \sigma_1^2, \rho_1)$ equal to $(1, 0.9, 0.02, 0.9)$.

We examined six coefficient regression functions displayed in Figure 1: (1) $\beta(\tau) = 0.5$, (2) $\beta(\tau) = \tau$, (3) $\beta(\tau) = 1.5\tau^2$, (4) $\beta(\tau) = \frac{4}{3}\tau I(\tau < 0.5) + \frac{2}{3}I(\tau \geq 0.5)$, (5) $\beta(\tau) = \exp(-\frac{\tau^2}{0.328})$, and (6) $\beta(\tau) = -\tau + 1$. These six functions include three types of effects (constant, increasing, and decreasing). We note that $\int_0^1 \beta(\tau) d\tau$ equals to 0.5 under all scenarios, and this quantity is interpreted as the effect of exposures associated with the exposure distribution shifted to the right by one unit (i.e., the mean is increased by one

unit). Based on simulated quantile functions $Q_i(\tau)$, 100 health datasets were generated for each of different forms of $\beta(\tau)$ while fixing $\beta_0 = -3.5$. The conventional “mean” model using the mean of individual exposures at each time point as the covariate was also fitted for the comparison.

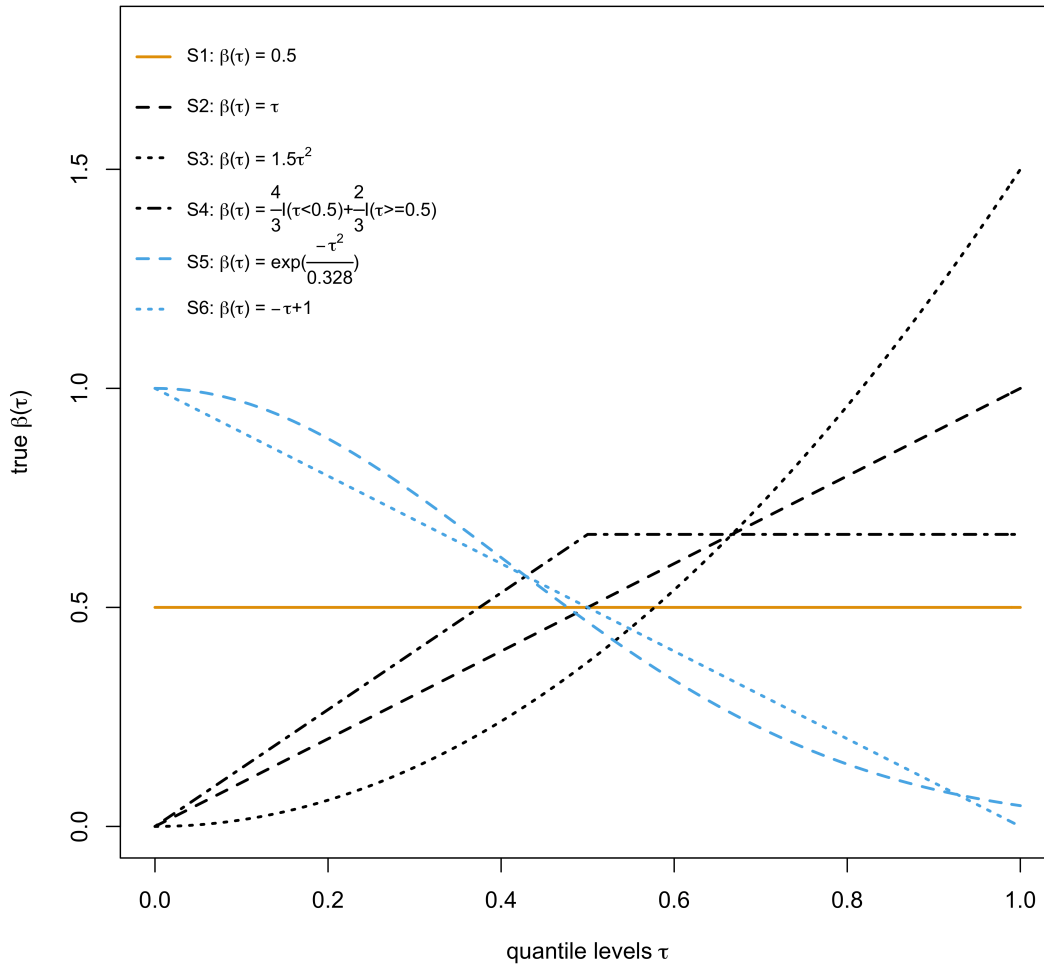


Figure 1: True coefficient regression functions $\beta(\tau)$ specified for the simulation study

Three quantities were used for performance evaluation: (a) the effect associated with the exposure distribution shifted to the right by one unit, which is measured by $\int \beta(\tau)d\tau$ for the proposed model and parameter α for the mean model; (b) predictive values of the exposure which is measured by $\int_0^1 \beta(\tau)Q_i(\tau)d\tau$ and $\alpha\mu_i$ for the proposed and mean models,

respectively; (c) the total number of exposure-attributable events, which is computed as $\sum_{i=1}^n \xi \{ \exp [\beta_0 + \int_0^1 \beta(\tau) Q_i(\tau) d\tau] - \exp(\beta_0) \}$ and $\sum_{i=1}^n \xi [\exp(\beta_0 + \alpha \mu_i) - \exp(\beta_0)]$ for the proposed and mean models, respectively. For these quantities, their relative bias, mean squared error (MSE), and 95% coverage probability (CP) were computed.

For $\int_0^1 \beta(\tau) d\tau$ and the total number of exposure-attributable events, their relative bias, MSE, and CP were computed by averaging over simulations. However, for predictive values, we averaged over both simulations and time points. Specifically, when exposure quantile functions were estimated, the MSE of predictive values of the exposure was calculated as:

$$\frac{1}{n \times D} \sum_{i=1}^n \sum_{d=1}^D \left[\int_0^1 \hat{\beta}^{(d)}(\tau) \hat{Q}_i^{(d)}(\tau) d\tau - \int_0^1 \beta(\tau) Q_i(\tau) d\tau \right]^2 \quad (8)$$

for the proposed model, where subscript d is the index for the simulation with $n = 1000$ and $D = 100$; $\hat{\beta}^{(d)}(\tau) = \hat{\boldsymbol{\beta}}^{(d)T} \mathbf{K}(\tau)$, $\hat{\boldsymbol{\beta}}^{(d)}$ is the vector of estimated basis coefficients defined in Eqn. (4); $\hat{Q}_i(\tau)^{(d)} = \mathbf{B}(\tau)^T \hat{\boldsymbol{\theta}}_{\cdot,i}^{(d)}$, $\hat{\boldsymbol{\theta}}_{\cdot,i}^{(d)}$ are estimated basis coefficients defined in Eqn. (7). The computation of the relative bias and CP follows a similar manner.

Additionally, the estimation performance of $\beta(\tau)$ was examined with respect to its bias, MSE, and CP by averaging over simulations and quantile levels $\tau_j \in \{0, 0.01, \dots, 0.99, 1\}$. For example, MSE of $\beta(\tau)$ is $1/(J \times D) \sum_{j=1}^J \sum_{d=1}^D [\hat{\boldsymbol{\beta}}^{(d)T} \mathbf{K}(\tau_j) - \beta(\tau_j)]^2$. Relative bias was not computed, since $\beta(\tau)$ can take value of 0.

In this simulation study, we modeled $\beta(\tau)$ using orthonormal Bernstein polynomials of degree two (i.e., three basis functions) and specified vague normal priors $N(0,100)$ for the corresponding basis coefficients. The over-dispersion parameter included in the health model was updated using Metropolis-Hastings (MH) algorithms with an uniform prior. For the estimation of exposure quantile functions, we used four piecewise Gamma functions to expand quantile functions. Coefficients $\theta_{0,i}$ and $\theta_{l,i}^*$ were assigned $N(0, 100)$ priors and were

updated using MH algorithms; σ_0^2 and σ_1^2 were given InvGamma(0.1, 0.1) priors and were updated using Gibbs sampling; discrete priors (i.e., 1000 equally spaced values between 0 and 1) were assigned for ρ_0 and ρ_1 which were updated using MH algorithms. We generated 10,000 MCMC samples and discarded the first 5,000 samples as burn-in when estimating quantile functions; while 5,000 samples were generated and the first 2,500 samples were discarded as burn-in when estimating health effects regardless of using true or estimated quantile functions.

Simulation results from using different exposure covariates (true mean exposures, true exposure quantile functions, and estimated quantile functions) are summarized in Table 1. We first focus on the case where exposure quantile functions and mean exposures are assumed to be known. Under the scenario where $\beta(\tau)$ is a constant (i.e., S1), results from using quantile functions and mean of exposures are similar. Since $\beta(\tau)$ was modeled using the basis expansion, a larger MSE was observed for the proposed model. For other scenarios, the proposed model resulted in empirically unbiased estimates of health effects. However, we observed biased estimates of health effects when using mean exposures. Specifically, we found positive biases when the upper tail of exposure distributions has larger effects (e.g., S2 and S3), and negative biases when the effects decrease as the quantile level increases (e.g., S5 and S6). The reverse pattern was observed for the total number of events attributed to exposures and predictive values of exposures. In S4 where the health effect first increases and then becomes a constant, the model using mean exposure happened to lead to a nearly unbiased estimate with conservative 95% credible intervals (CIs) for $\int_0^1 \beta(\tau)d\tau$. However, this model failed to characterize effects of exposures as indicated by the larger MSE and severe under-coverage associated with predictive values of exposures. It is also worth noting that the proposed model performed slightly worse in this scenario, for example, the MSE

of $\int_0^1 \beta(\tau) d\tau$ was higher than S2, S3, and S5, likely because $\beta(\tau)$ in S4 is approximated less well by the basis expansion.

Table 1: Simulation results using different exposure covariates

Scenario	Covariate ^a	$\int_0^1 \beta(\tau) d\tau$ ^b			$\beta(\tau)$			predictive values of exposures			exposure-attributable events		
		relative bias	relative MSE ^c	CP (%)	bias	MSE	CP (%)	relative bias	relative MSE ^c	CP (%)	relative bias	relative MSE ^c	CP (%)
S1	mean	0.004	1.00	94	-	-	-	0.004	1.000	94.00	0.001	1.000	95
	quantile	0.005	1.10	96	0.002	0.016	93.70	-0.002	3.889	93.39	0.000	1.069	95
	quantile with errors	0.011	1.47	92	0.004	0.031	95.48	0.004	6.475	96.41	0.001	1.101	94
S2	mean	0.009	1.00	89	-	-	-	-0.122	1.000	0.01	-0.008	1.000	83
	quantile	-0.002	0.80	96	-0.001	0.015	92.17	-0.002	0.052	93.66	-0.000	0.610	93
	quantile with errors	0.010	1.07	91	0.003	0.032	93.13	0.010	0.108	95.50	0.000	0.620	93
S3	mean	0.019	1.00	75	-	-	-	-0.174	1.000	0.00	-0.010	1.000	82
	quantile	-0.001	0.39	97	-0.000	0.013	92.92	-0.003	0.023	91.74	0.000	0.408	96
	quantile with errors	0.014	0.74	90	0.005	0.036	90.47	0.017	0.056	94.12	0.001	0.398	96
S4	mean	0.003	1.00	100	-	-	-	-0.081	1.000	0.04	-0.006	1.000	89
	quantile	-0.001	1.01	98	-0.001	0.014	93.61	0.003	0.127	93.56	0.000	0.751	95
	quantile with errors	0.008	1.38	98	0.001	0.039	90.57	0.015	0.302	94.82	0.001	0.759	94
S5	mean	-0.010	1.00	95	-	-	-	0.182	1.000	0.00	0.017	1.000	77
	quantile	0.002	0.80	95	0.001	0.018	95.90	-0.003	0.057	95.73	0.000	0.361	95
	quantile with errors	0.003	0.85	97	0.000	0.033	97.12	-0.002	0.107	96.02	-0.000	0.381	95
S6	mean	-0.011	1.00	94	-	-	-	0.163	1.000	0.02	0.014	1.000	80
	quantile	0.000	0.75	95	0.000	0.016	95.74	-0.001	0.075	95.67	-0.001	0.537	95
	quantile with errors	0.002	0.83	96	0.000	0.042	94.42	-0.003	0.127	95.89	-0.002	0.586	93

^a mean = true mean exposures, quantile = true exposure quantile functions, quantile with errors = estimated exposure quantile functions.

^b For the model using mean exposure as the exposure covariate, the parameter α was reported.

^c Relative MSE was computed by treating the model using the true mean exposure as the reference.

We also evaluated the decision to select the proposed model over the conventional “mean” exposure model informed by the widely available information criterion (WAIC) (?). Among 100 simulations, the proportion of simulations in which the WAIC favored the

mean model is 82% under S1 where the mean model is a valid and better choice. While for other scenarios, the WAIC favored the proposed model over 95% of the time.

When exposure quantile functions were estimated from the simulated dataset containing individual-level exposures, we applied the two-stage estimation procedure to account for uncertainties of estimating exposure quantile functions. Figure 2(a) shows simulated exposure data over nine consecutive days where exposure distributions are right skewed and change over time smoothly. Estimated quantile functions traced the truth well as shown in Figure 2(b). Compared to the case where true quantile functions were used, MSE of those four quantities were increased (Table 1). However, across all scenarios, coverage probabilities still achieved or were close to the nominal level. We found that without accounting for estimation uncertainties by using the posterior means of the estimated quantile functions can lead to bias and under-coverage (results are not shown).

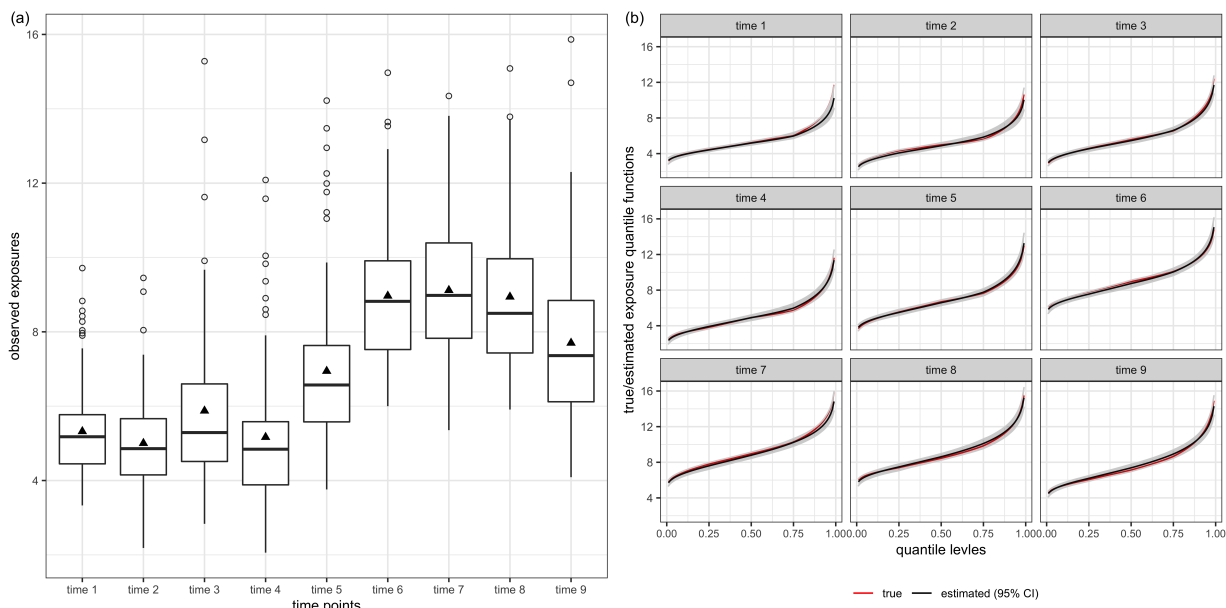


Figure 2: (a) boxplots of exposures observed on nine consecutive days in the simulated data, (b) true/estimated exposure quantile functions for nine consecutive days

5 Real Data Analysis

In this section, we analyzed the motivating data introduced in Section 2 using both the proposed scalar-on-quantile-function model and the conventional model using average concentrations of air pollutants as the exposure.

5.1 Estimation of daily exposure quantile functions

Distributions of four air pollutants from SHEDS at one representative ZCTA are presented in Figures 3(a)-(d). We observed different degrees of skewness in exposure distributions for all four air pollutants. We noted that distributions of CO and EC are very different across days compared to NO_x and PM_{2.5}. Hence, for estimating quantile functions, quantile functions of CO and EC were assumed to be independent across days and ZCTAs, while temporal correlations were introduced for quantile functions of NO_x and PM_{2.5}. In this analysis, we used the same priors, the number of MCMC iterations, and burn-in as in Section 4. Figures 3(e)-(h) shows the corresponding empirical quantile and estimated quantile functions from using four piecewise Gamma functions. Overall, our use of basis functions sufficiently capture exposure distributions with larger uncertainties in lower and upper tails as expected.

5.2 Estimation of health effects for ED visits

Associations between ED visits and same-day air pollution concentrations were examined using the proposed model with estimated quantile functions and uncertainty propagation, and the conventional model using sample mean of individual exposures at the ZCTA level. Following the previous health analysis (Sarnat et al., 2013), the following confounders were controlled for in all models: non-linear effect of year-specific temporal trends using day

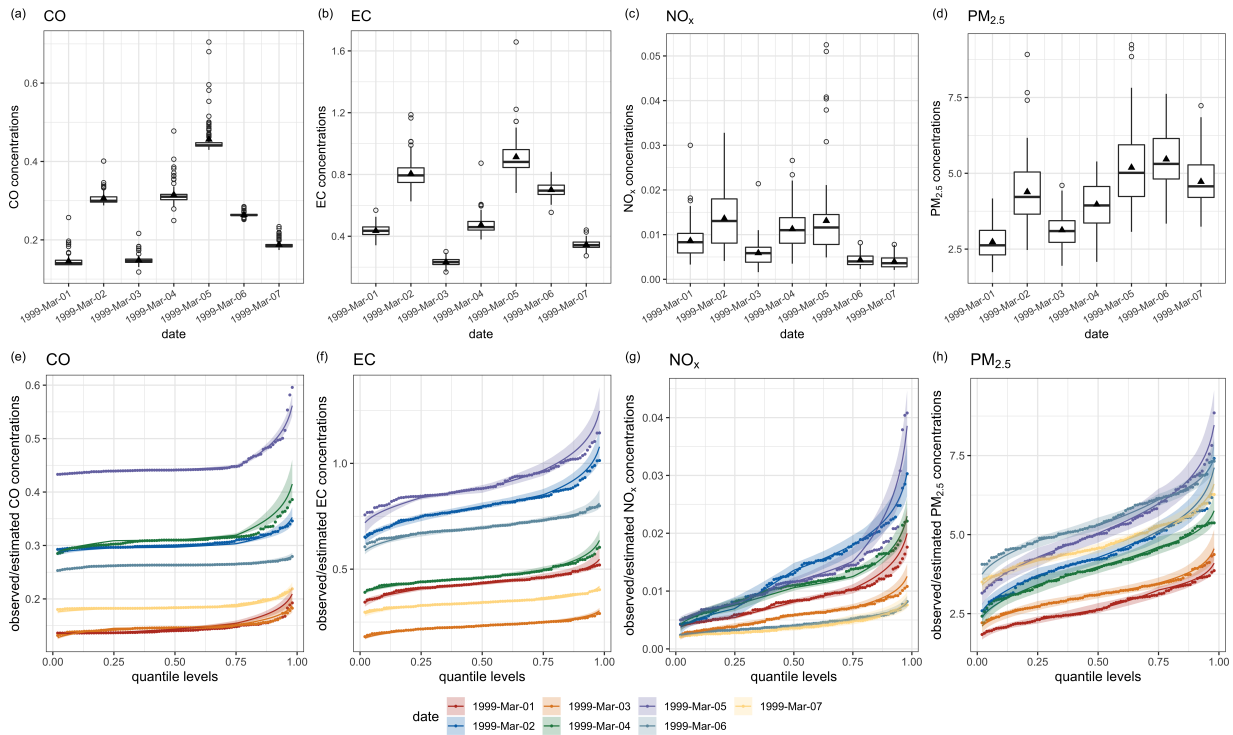


Figure 3: (a)-(d) Boxplots of concentrations of air pollutants obtained from SHEDS at ZCTA 30032 on seven representative days, (e)-(h) empirical/estimated quantile functions with 95% credible intervals of air pollutants obtained from SHEDS at ZCTA 30032 on seven representative days (empirical quantile functions are denoted by solid points).

of year, non-linear effect of same-day dew-point temperature, indicators of day of week, an indicator of federal holidays, non-linear effect of 3-day moving average of minimum temperature (maximum temperature was controlled for cardiovascular disease ED visits). All non-linear effects were modeled with natural cubic splines with four degrees of freedom. Exchangeable ZCTA-specific random intercepts were included for all models. We varied the number of basis functions used for modeling $\beta(\tau)$ from two to three, and results from the model with lower WAIC are reported. The same priors as in Section 4 were introduced for basis coefficients and the over-dispersion parameter; the variance parameter of spatial random effects were assumed to have $\text{InvGamma}(0.1, 0.1)$ prior. We ran for 7,500 iterations, the first 3,500 being discarded as burn-in.

Figure 4 plots the estimated $\beta(\tau)$ with 95% CIs for different combinations of air pollutants and causes of ED visits. We observed that the WAIC clearly favors the proposed model under some cases (e.g., panels (b), (c), (e), (f), and (h) of Figure 4). For example, Figure 4(e) shows that lower and upper tails of the distribution of EC concentrations have larger effects on respiratory disease ED visits. The resulting percent (%) increase in risk associated with one unit shift to right for the distribution of EC concentrations is estimated to be 2.58 (95% CI: 0.82 - 4.31) and 0.56 (95% CI: -0.14 - 1.26) using the proposed and the conventional models, respectively. In some cases, the WAIC indicates that the model utilizing quantile functions and the model using sample mean of exposures fitted the data equally. For example, Figure 4(j) shows that estimates of health effects of $\text{PM}_{2.5}$ on asthma or wheeze ED visits basically remain the same across quantile levels, matching the estimate obtained from the mean model. Estimates of percent increase in risk for the rest of combinations are presented in Table S1.

Figures 5(a)-(d) display estimated quantile functions where their corresponding expo-

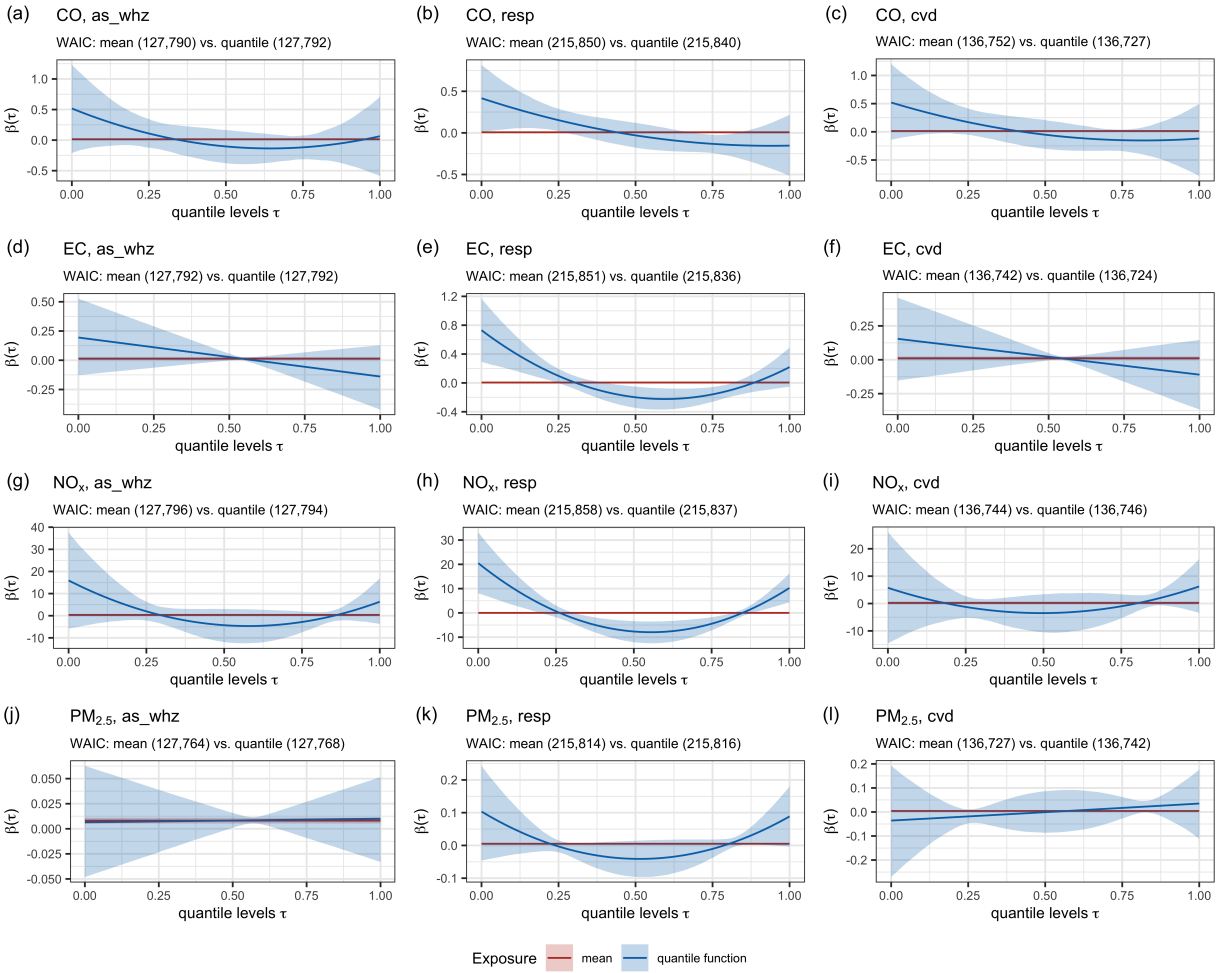


Figure 4: Estimates of $\beta(\tau)$ with 95% credible intervals from analyzing the motivating data (as_whz = asthma or wheeze ED visits, resp = respiratory disease ED visits, cvd = cardiovascular disease ED visits).

sure medians are at the 25th, 50th, 75th, and 95th percentiles of the estimated medians across all ZCTAs and days. Dashed horizontal lines mark mean exposure calculated from SHEDS data used for estimating the quantile functions. These quantile functions were selected to represent different exposure contrasts across ZCTAs and days. Estimates of relative risks associated with changes in selected estimated quantile functions from the proposed and the conventional models are shown in Figures 5(e)-(h). Two contrasts were selected to represent different exposure effects: (1) comparing quantile functions with medians at the 75th and 25th percentiles to represent typical exposure contrast, and (2) comparing quantile functions with medians at the 95th and 50th percentiles to represent more extreme exposure effects.

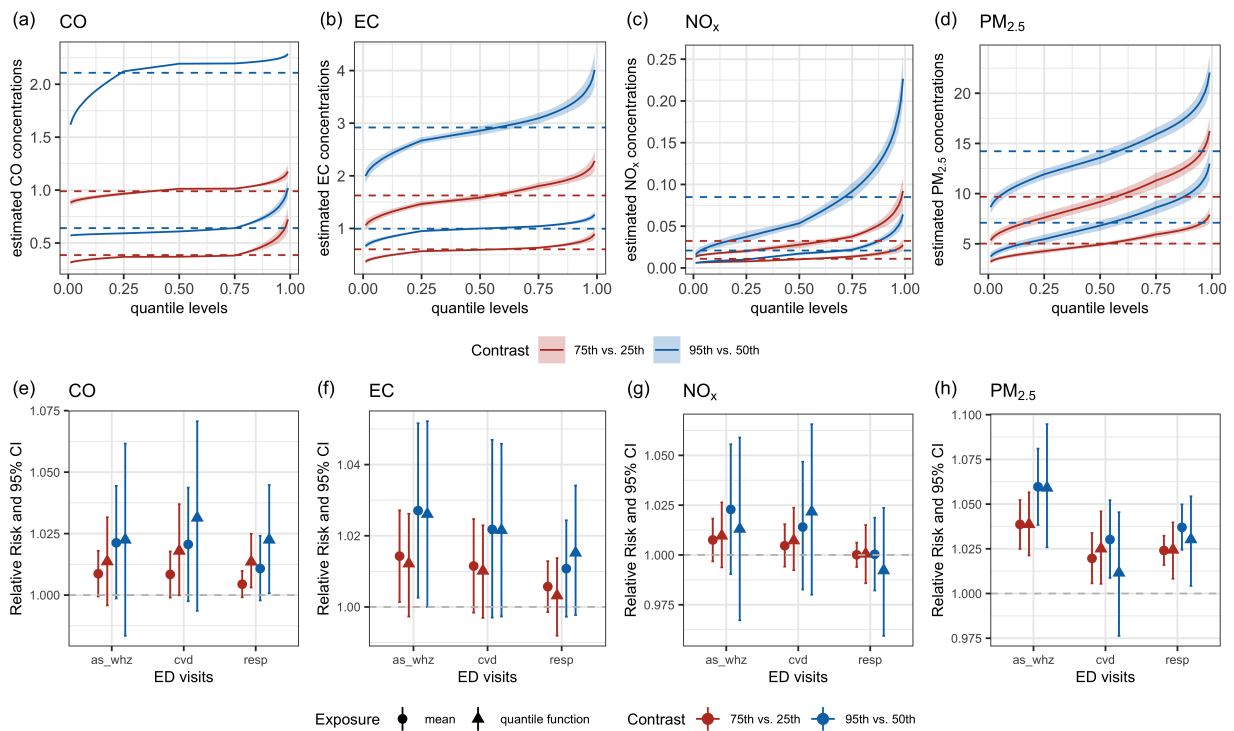


Figure 5: Short-term associations between ED visits associated with two observed exposure distributions defined by the exposure median (75th versus 25th, and 95th versus 50th percentiles of the distribution of estimated medians across all ZCTAs and days). Results obtained from models using the mean concentrations as the exposure are also shown. as_whz = asthma or wheeze, resp = respiratory disease, cvd = cardiovascular disease.

For short-term associations between ambient concentrations of CO and respiratory ED

visits and cardiovascular disease ED visits, as shown in Figures 4(b) and (c), the proposed model including quantile functions was preferred, and we found that effects of CO at lower quantile levels are more pronounced. The corresponding short-term associations for the two selected contrasts are presented in Figure 5(e). We observed that simply using average concentrations of CO as the covariate in the health model underestimated relative risk of CO on cardiovascular disease ED visits and respiratory disease ED visits compared with the proposed model that considers the entire exposure distributions. Differences in the estimated number of ED visits attributed to the exposure to air pollution are also present. For example, Figures 6(a)-(b) illustrates differences in the number of exposure-attributable ED visits by ZCTA when effects of air pollutants vary by their quantile levels. Specifically, the total number of cardiovascular ED visits attributed to CO exposure was estimated to be 798 (95% CI: 74 - 3,240) using the proposed model, while the mean model yielded an estimate of 640 (95% CI: -80 - 1,343). In contrast, for PM_{2.5} and asthma or wheeze ED visits where health effects are invariant with respect to quantile levels, the proposed model and the conventional model led to similar results (Figure 6(c)).

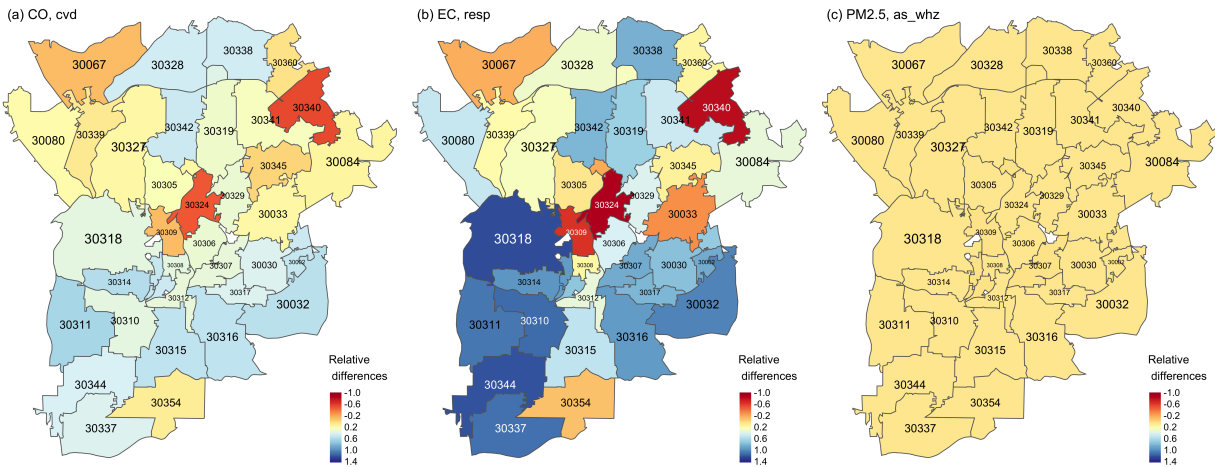


Figure 6: Relative differences of the ZCTA-level number of exposure-attributable ED visits between using the proposed exposure-quantile model and the conventional mean-exposure model (as_whz = asthma or wheeze ED visits, resp = respiratory disease ED visits, cvd = cardiovascular disease ED visits).

6 Discussion

In this work, we propose a scalar-on-quantile-function approach to fully characterize effects of environmental exposures on aggregate health outcomes by treating exposure quantile functions as functional covariates. Compared to methods which solely include summary statistics of personal exposures as the exposure metric of interest, our approach accounts for within-group exposure heterogeneity and allows more flexible associations between exposures and aggregate health outcomes. In addition, parametric distribution assumptions on exposure distributions are not necessary in our approach. With the proposed Bayesian two-stage estimation procedure, estimates of health effects can be obtained while incorporating uncertainties in the estimation of exposure quantile functions. This two-stage procedure also alleviates the computation burden when associations between one exposure and multiple health outcomes are examined, compared to approaches that jointly model exposure and health data.

Applying the proposed model to the motivating ED visits data in Atlanta, we identified novel short-term associations between ambient air pollution concentrations and ED visits which were masked when daily population average exposures were linked to ED visits. For example, results suggest that effects of ambient concentrations of CO on respiratory disease ED visits and cardiovascular disease ED visits are highest at lower quantile levels. These new findings may be important for identifying subpopulations most vulnerable to ambient air pollution. For the majority of pollutant and outcome pairs, we found robust and positive associations comparable to the conventional approach, which strengthens prior evidence on the negative health effects of air pollution.

The proposed model was motivated by the SHEDS data which provide simulated personal exposure to different air pollutants in Atlanta over four years. While personal ex-

posures are not widely available in large scale population-based epidemiological studies, the proposed model can be applied to more general settings. Specifically, the proposed approach is applicable for scenarios where within group exposure heterogeneity exists and can be characterized using quantile functions. For example, in the scenario where environmental exposures are predicted using spatial-temporal models at finer spatial resolutions compared to spatial resolution of the health data, our proposed approach can be applied with exposure quantile functions derived from predicted exposures and population density. In addition, the health outcome does not have to be restricted to aggregated counts. For example, in the application of analyzing birthweight data in North Carolina conducted by Berrocal et al. (2011), the effects of an individual's exposure distribution can be assessed using our approach.

In this work, we focus on single environmental exposure. One further extension of the proposed approach is to simultaneously examine effects of multiple exposures on aggregate health outcome. A possible strategy is to incorporate quantile surface of exposures as the functional predictor in the health model, which might account for correlations between exposures. In the real data analysis, we found that the estimation of exposure quantile functions is sensitive to outliers. As a result, larger uncertainties of estimated quantile functions are observed in the distribution tails and the estimation of health effects may be affected. To mitigate the impact of outliers on the exposure quantile estimation, one could consider introducing parametric methods for characterizing tails of exposure distributions (Zhou et al., 2012).

7 Acknowledgements

We thank Lisa Baxter and Kathie Dionisio from the US EPA for providing the SHEDS exposure data.

References

- Alhanti, B. A., Chang, H. H., Winqvist, A., Mulholland, J. A., Darrow, L. A., and Sarnat, S. E. (2016). Ambient air pollution and emergency department visits for asthma: a multi-city assessment of effect modification by age. *Journal of exposure science & environmental epidemiology*, 26(2):180–188.
- Bekkar, B., Pacheco, S., Basu, R., and DeNicola, N. (2020). Association of air pollution and heat exposure with preterm birth, low birth weight, and stillbirth in the us: a systematic review. *JAMA network open*, 3(6):e208243–e208243.
- Bellucci, M. A. (2014). On the explicit representation of orthonormal bernstein polynomials. *arXiv preprint arXiv:1404.2293*.
- Berrocal, V. J., Gelfand, A. E., Holland, D. M., Burke, J., and Miranda, M. L. (2011). On the use of a pm_{2.5} exposure simulator to explain birthweight. *Environmetrics*, 22(4):553–571.
- Bhaskaran, K., Gasparrini, A., Hajat, S., Smeeth, L., and Armstrong, B. (2013). Time series regression studies in environmental epidemiology. *International journal of epidemiology*, 42(4):1187–1195.
- Boogaard, H., Walker, K., and Cohen, A. J. (2019). Air pollution: the emergence of a major global health risk factor. *International health*, 11(6):417–421.

- Burke, J. M., Zufall, M. J., and OeZKAYNAK, H. (2001). A population exposure model for particulate matter: case study results for pm_{2.5} in philadelphia, pa. *Journal of Exposure Science & Environmental Epidemiology*, 11(6):470–489.
- Calder, C. A., Holloman, C. H., Bortnick, S. M., Strauss, W., and Morara, M. (2008). Relating ambient particulate matter concentration levels to mortality using an exposure simulator. *Journal of the American Statistical Association*, 103(481):137–148.
- Carroll, R. J., Ruppert, D., Stefanski, L. A., and Crainiceanu, C. M. (2006). *Measurement error in nonlinear models: a modern perspective*. Chapman and Hall/CRC.
- Chang, H. H., Fuentes, M., and Frey, H. C. (2012). Time series analysis of personal exposure to ambient air pollution and mortality using an exposure simulator. *Journal of exposure science & environmental epidemiology*, 22(5):483–488.
- Comess, S., Chang, H. H., and Warren, J. L. (2022). A bayesian framework for incorporating exposure uncertainty into health analyses with application to air pollution and stillbirth. *arXiv preprint arXiv:2203.16627*.
- Dionisio, K. L., Isakov, V., Baxter, L. K., Sarnat, J. A., Sarnat, S. E., Burke, J., Rosenbaum, A., Graham, S. E., Cook, R., Mulholland, J., et al. (2013). Development and evaluation of alternative approaches for exposure assessment of multiple air pollutants in atlanta, georgia. *Journal of Exposure Science & Environmental Epidemiology*, 23(6):581–592.
- Dominici, F., Zeger, S. L., and Samet, J. M. (2000). A measurement error model for time-series studies of air pollution and mortality. *Biostatistics*, 1(2):157–175.
- Goldman, G. T., Mulholland, J. A., Russell, A. G., Srivastava, A., Strickland, M. J., Klein,

- M., Waller, L. A., Tolbert, P. E., and Edgerton, E. S. (2010). Ambient air pollutant measurement error: characterization and impacts in a time-series epidemiologic study in atlanta. *Environmental science & technology*, 44(19):7692–7698.
- Guo, Y., Gasparrini, A., Armstrong, B. G., Tawatsupa, B., Tobias, A., Lavigne, E., Coelho, M. d. S. Z. S., Pan, X., Kim, H., Hashizume, M., et al. (2017). Heat wave and mortality: a multicountry, multicomunity study. *Environmental health perspectives*, 125(8):087006.
- Huang, G., Lee, D., and Scott, E. M. (2018). Multivariate space-time modelling of multiple air pollutants and their health effects accounting for exposure uncertainty. *Statistics in medicine*, 37(7):1134–1148.
- Jenkins, P. (1996). Personal exposure to airborne particles and metals: results from the particle team study in riverside, california. *Journal of Exposure Analysis and Environmental Epidemiology*, 6(1):57.
- Jerrett, M., Arain, A., Kanaroglou, P., Beckerman, B., Potoglou, D., Sahuvaroglu, T., Morrison, J., and Giovis, C. (2005). A review and evaluation of intraurban air pollution exposure models. *Journal of Exposure Science & Environmental Epidemiology*, 15(2):185–204.
- Jerrett, M., Burnett, R. T., Kanaroglou, P., Eyles, J., Finkelstein, N., Giovis, C., and Brook, J. R. (2001). A gis–environmental justice analysis of particulate air pollution in hamilton, canada. *Environment and Planning A*, 33(6):955–973.
- Landrigan, P. J. (2017). Air pollution and health. *The Lancet Public Health*, 2(1):e4–e5.
- Lee, D., Mukhopadhyay, S., Rushworth, A., and Sahu, S. K. (2017). A rigorous statisti-

- cal framework for spatio-temporal pollution prediction and estimation of its long-term impact on health. *Biostatistics*, 18(2):370–385.
- Leiva, V., Barros, M., Paula, G. A., and Sanhueza, A. (2008). Generalized birnbaum-saunders distributions applied to air pollutant concentration. *Environmetrics: The official journal of the International Environmetrics Society*, 19(3):235–249.
- Manisalidis, I., Stavropoulou, E., Stavropoulos, A., and Bezirtzoglou, E. (2020). Environmental and health impacts of air pollution: a review. *Frontiers in public health*, page 14.
- Neelon, B. (2019). Bayesian zero-inflated negative binomial regression based on pólya-gamma mixtures. *Bayesian analysis*, 14(3):829.
- Özkaynak, H., Xue, J., Weker, R., Butler, D., and Koutrakis, P. (1996). Particle team (pteam) study: Analysis of the data. final report, volume 3. Technical report, Harvard Univ., Boston, MA (United States). School of Public Health.
- Polson, N. G., Scott, J. G., and Windle, J. (2013). Bayesian inference for logistic models using pólya-gamma latent variables. *Journal of the American statistical Association*, 108(504):1339–1349.
- Reich, B. J. (2012). Spatiotemporal quantile regression for detecting distributional changes in environmental processes. *Journal of the Royal Statistical Society: Series C (Applied Statistics)*, 61(4):535–553.
- Reich, B. J., Fuentes, M., and Burke, J. (2009). Analysis of the effects of ultrafine particulate matter while accounting for human exposure. *Environmetrics: The official journal of the International Environmetrics Society*, 20(2):131–146.

- Richardson, S. and Best, N. (2003). Bayesian hierarchical models in ecological studies of health–environment effects. *Environmetrics: The official journal of the International Environmetrics Society*, 14(2):129–147.
- Richmond-Bryant, J. and Long, T. C. (2020). Influence of exposure measurement errors on results from epidemiologic studies of different designs. *Journal of Exposure Science & Environmental Epidemiology*, 30(3):420–429.
- Sarnat, S. E., Sarnat, J. A., Mulholland, J., Isakov, V., Özkaynak, H., Chang, H. H., Klein, M., and Tolbert, P. E. (2013). Application of alternative spatiotemporal metrics of ambient air pollution exposure in a time-series epidemiological study in atlanta. *Journal of exposure science & environmental epidemiology*, 23(6):593–605.
- Sheppard, L. (2003). Insights on bias and information in group-level studies. *Biostatistics*, 4(2):265–278.
- Steinle, S., Reis, S., and Sabel, C. E. (2013). Quantifying human exposure to air pollution—moving from static monitoring to spatio-temporally resolved personal exposure assessment. *Science of the Total Environment*, 443:184–193.
- Steinle, S., Reis, S., Sabel, C. E., Semple, S., Twigg, M. M., Braban, C. F., Leeson, S. R., Heal, M. R., Harrison, D., Lin, C., et al. (2015). Personal exposure monitoring of pm_{2.5} in indoor and outdoor microenvironments. *Science of the Total Environment*, 508:383–394.
- Sugg, M. M., Fuhrmann, C. M., and Runkle, J. D. (2018). Temporal and spatial variation in personal ambient temperatures for outdoor working populations in the southeastern usa. *International journal of biometeorology*, 62(8):1521–1534.

- Thornton, P., Thornton, M., Mayer, B., Wei, Y., Devarakonda, R., Vose, R., and Cook, R. (2016). Daymet: daily surface weather data on a 1-km grid for north america, version 3. ornl daac, oak ridge, tennessee, usa. *USDA-NASS, 2019. 2017 Census of Agriculture, Summary and State Data, Geographic Area Series, Part 51, AC-17-A-51*.
- Yoo, E.-h., Eum, Y., Roberts, J. E., Gao, Q., and Chen, K. (2021). Association between extreme temperatures and emergency room visits related to mental disorders: A multi-region time-series study in new york, usa. *Science of The Total Environment*, 792:148246.
- Zhou, J., Chang, H. H., and Fuentes, M. (2012). Estimating the health impact of climate change with calibrated climate model output. *Journal of agricultural, biological, and environmental statistics*, 17(3):377–394.
- Zidek, J. V., Shaddick, G., Meloche, J., Chatfield, C., and White, R. (2007). A framework for predicting personal exposures to environmental hazards. *Environmental and Ecological Statistics*, 14(4):411–431.
- Zidek, J. V., Shaddick, G., White, R., Meloche, J., and Chatfield, C. (2005). Using a probabilistic model (pcnem) to estimate personal exposure to air pollution. *Environmetrics: The official journal of the International Environmetrics Society*, 16(5):481–493.

8 Funding

The work is supported by grant R01ES027892 and R01ES028346 from the National Institutes of Environmental Health. The content is solely the responsibility of the authors and does not necessarily represent the official views of the National Institutes of Health.